Available online at www.sciencedirect.com
SCIENCE DIRECT®
Materials Chemistry and Physics 92 (2005) 197–204
MATERIALS CHEMISTRY AND PHYSICS
www.elsevier.com/locate/matchemphys

Structure and properties of Cr promoted VPO catalysts

Beatriz T. Pierini, Eduardo A. Lombardo *

Instituto de Investigaciones en Catálisis y Petroquímica, INCAPE (FIQ-UNL, CONICET), Santiago del Estero 2829, 3000 Santa Fe, Argentina

Received 13 October 2004; received in revised form 3 January 2005; accepted 11 January 2005

Abstract

In this work, $VOHPO_4 \cdot 1/2H_2O$ was synthesized from V_2O_5 and anhydrous H_3PO_4 in an alcohol mixture. The $Cr(NO_3)_3$ in varying proportions was either added during synthesis or impregnated on the dried vanadyl hydrogen phosphate. The solid features and the catalytic behavior of these formulations were affected by both the addition procedure and the Cr load. The effect of Cr upon the catalyst structure and the development of acid and redox sites were studied through XRD, TPR, LRS and FT-IR. Acetonitrile was used as a probe molecule to ascertain the Lewis acid strength of the surface sites present in all the VPO formulations. It is concluded that the impregnation of Cr is more effective to increase the concentration of very strong Lewis acid sites, while this method and co-precipitation are similarly effective in the generation of V^{5+}/V^{4+} redox couples. Both types of sites in adequate balance are needed to optimize the catalytic behavior of VPO formulations.

Keywords: Cr promoter; VPO catalysts; Maleic anhydride; Selective oxidation; Acidity

1. Introduction

The mixed oxide of P and V (VPO) is the only solid that successfully catalyzes the selective oxidation of *n*-butane to maleic anhydride. The molar yield of this process is roughly 60%. To increase this yield many promoters have been tried and in fact used in industrial practice. However, little is known about the mode of action of the promoters, for example, how they affect the structure, acidity and redox ability of the solid system.

Cr is an attractive candidate because its size, electronegativity, "d" character and multiple oxidation states may be suitable to modify the catalytic behavior of the VPO in the desired direction of increased yield. The predominant crystalline phase in VPO is $(VO)_2P_2O_7$. Its oxidation to β-$VOPO_4$ is known to be deleterious to the selectivity to maleic anhydride. So, one role of Cr^{3+} could be to protect V^{4+} from overoxidation. Additionally, $CrPO_4$ could be formed and intercalated in the pyrophosphate matrix, helping to retain the excess phosphorous always present in the industrial catalyst. In fact, this has been claimed to be the case when Co was added to VPO formulations [1,2]. The presence of chromium may also affect the acidity of the base VPO. And this is catalytically important for the rate-determining step in the activation of the paraffin since the C–H bond breaking requires the presence of strong surface Lewis acid sites. It is widely accepted that *n*-butane adsorbs on the Lewis site and on an adjacent V=O center from the [2 0 0] plane of the $(VO)_2P_2O_7$ structure [3,4]. The paraffin interacts through the methylenic groups and after reaction 2-butene is formed and water released. The reduced surface is then reoxidized by gas phase oxygen to re-start the catalytic cycle.

The Lewis sites may be affected in strength and/or number by the promoter. In this regard, note that Cr is a well-performing catalyst for the oxydehydrogenation and dehydrogenation of C_1–C_4 paraffins [5,6]. In this system the breaking of the C–H bond takes center stage again.

McCormick et al. [5] used VPO solids promoted by Cr and Fe for the partial oxidation of methane. They reported high selectivity to formaldehyde at low methane conversion. The addition of either promoter affected the catalytic behavior. The presence of α_{II}-$VOPO_4$ (V^{5+}) was documented through XRD. The average oxidation state of vanadium in the

* Corresponding author. Tel.: +54 342 4586831; fax: +54 342 4536861.
E-mail address: nfisico@fiqus.unl.edu.ar (E.A. Lombardo).

0254-0584/$ – see front matter © 2005 Elsevier B.V. All rights reserved.
doi:10.1016/j.matchemphys.2005.01.009

promoted formulations was higher than 4 (ca. 4.1) calculated from NMR measurements. At surface level, the XPS data indicated an average oxidation state of 4.4. They concluded that in their case the role of the promoters was to favor the development of V^{5+} containing phases. They also concluded that $CrPO_4$ was likely to be present in their catalysts. They supported this statement with XPS and IR spectroscopy data. Concerning the latter, they reported an increasing intensity of the 795 cm^{-1} band upon Cr addition. This band corresponded to the vibration of the long bond between one [2 0 0] plane and the next (V=O)–O. The intensity of this band varied with the separation of the layers that in turn were affected by the intercalation of Cr. However, this effect and/or the appearance of the V^{5+} phase were not substantiated by XRD.

In other hand, Harrouch Batis and coworkers [7] studied the effect of the addition of Cr to VPO upon catalytic behavior in the selective oxidation of *n*-butane and reported that Cr had no beneficial effect. However, Hutchings [8,9] reported that the addition of Cr (Cr/V = 0.03) increased the surface area, the activity and the selectivity of the catalyst.

The potential ability of Cr to improve desirable properties of the VPO system and the paucity and contradictory data available in the open literature were the driving force behind this systematic study of the effect of Cr addition to VPO solids. Two different methods of preparation were used and several techniques were tried to identify the mode of action of the promoter.

2. Experimental

2.1. Precursor synthesis

The precursor was obtained by reduction of 5 g of V_2O_5 with 30 ml of isobutanol and 20 ml of benzyl alcohol under reflux for 3 h. Orthophosphoric acid 100% was then added in the amount needed to obtain a P/V ratio of 1.3 and the solution refluxed for another 2 h. After completion of the reaction, the solid phase was recovered by filtration and dried in an oven at 150 °C overnight. This solid is named VPO, the unpromoted precursor.

Chromium (as $Cr(NO_3)_3{\cdot}9H_2O$) was incorporated in the following ways: (i) by addition, together with phosphoric acid (co-precipitated precursor). The nomenclature is Cr*x*c (where *x* represents wt.% of Cr and "c" the co-precipitation method); (ii) by precursor (VPO) impregnation Cr*x*i (where *x* represents wt.% of Cr and "i" the impregnation method). The impregnation solutions contained the required amount of chromium nitrate dissolved in isobutyl alcohol. After impregnation, the wet solid was dried at 150 °C in an oven overnight.

2.2. Catalyst activation and testing

A fixed-bed reactor containing 1.0 g of precursor with particle size in the range of 177–250 μm was used to activate the solids and perform the catalytic tests. All products were analyzed using an on-line gas chromatograph equipped with an FID detector and an AT-1200 column. The precursor was activated as follows: While flowing the reactant mixture (1.5% *n*-C_4H_{10} in air) at GHSV = 900 h^{-1}, the solid was heated at 3 °C min^{-1}, up to 280 °C, kept at this temperature for 3 h, and heated again to the temperature needed to achieve 80% conversion (∼380 °C). The system was kept under reaction conditions until no variation in both conversion and selectivity occurred (usually 48 h). At this point, the catalyst reached the steady state to measure its catalytic performance by varying temperature and space velocity as needed.

2.3. Precursor and catalyst characterization

2.3.1. Surface area

It was measured by N_2 adsorption (BET method) using a Quantachrome Nova 1000 sorptometer.

2.3.2. X-ray diffraction (XRD)

The measurements were made with a Shimadzu XD-D1 X-ray diffractometer, using nickel-filtered Cu Kα radiation with a scanning rate of 1 °C min^{-1}.

2.3.3. Temperature-programmed reduction (TPR)

The TPR experiments were performed in an Ohkura TP-20022S instrument equipped with a thermal conductivity detector (TCD); 100 mg of samples were used and the reducing gas was a 2% H_2–Ar stream, with a heating rate of 10 °C min^{-1} up to 800 °C.

2.3.4. Laser Raman spectroscopy (LRS)

The Raman spectra were recorded with a Jasco laser Raman spectrometer model TRS-600-SZ-P, equipped with a charge coupled device (CCD) with the detector cooled to about 153 K using liquid N_2. The excitation source was the 514.5 nm line of a Spectra 9000 Photometrics Ar ion laser. The laser power was set at 40 mW. All the spectra were recorded with the samples under ambient conditions. The powdered solid was pressed as a thin wafer about 1 mm thick.

2.4. Fourier transform infrared spectroscopy

The IR spectra were obtained using a Shimadzu FT-IR 8101 M spectrometer with a spectral resolution of 4 cm^{-1}. The solid samples were prepared in the form of pressed wafers (ca. 2 wt.% sample in KBr).

2.4.1. Acetonitrile adsorption

The samples for the adsorption experiments were prepared by compressing the used catalysts at 4 t cm^{-2} in order to obtain a self-supporting wafer. They were mounted on a transportable infrared cell with CaF_2 windows and external oven. The pretreatment was performed in a high-vacuum system. The sample was first outgassed at 450 °C for 12 h in a dynamic vacuum of 1.0×10^{-5} Torr. After cooling to room temperature, a spectrum of the catalyst wafer was

taken. After acetonitrile adsorption no bands were observed in the 1600 cm^{-1} region; therefore, no water was introduced during the adsorption of the base. Spectra were recorded in the presence of the gas phase and after evacuation of the cell at 30, 80, and 150 °C, for 10 min.

3. Results and discussion

3.1. VPO structure and catalytic behavior

All the precursors with or without Cr added showed a single crystalline phase: $VOHPO_4{\cdot}1/2H_2O$. The main phase present in the catalysts after activation and testing was $(VO)_2P_2O_7$, only Cr3.0c showed a mixture of V^{5+} and V^{4+} phases.

It is generally accepted that the active catalytic sites are located on the [2 0 0] plane of $(VO)_2P_2O_7$ [8]. This plane is generated from the [0 0 1] plane of the precursor. Several authors claim that it is possible to control the structure and morphology of the catalyst acting upon the synthesis procedures of the precursor [10–13]. The data shown in columns 3 and 4 of Table 1 do not support this claim for there is no correlation between the width of the key-related planes in the precursor and the catalyst. Note that the FWHM is directly connected with the lattice disorder perpendicular to these planes. In the same vein, columns 5 and 6 show no correlation in the extent of preferential exposure of the [0 0 1] and [2 0 0] planes.

The unit cell dimensions of the catalysts were calculated from the XRD data and are reported in Table 2. In all cases but one (Cr1.0c), the unit cell volume increases with the addition of Cr. In the impregnated series there is a monotonic increase in cell volume with increasing Cr load. The presence of Cr increases the surface area of all the catalysts (Table 3). However, there is no correlation between Cr load and surface area.

Table 3 shows the temperature needed to reach 80% conversion and the selectivity measured at the said conversion. Note that the addition of Cr leads to more active catalysts with no exception. In the impregnated series, there is an increase in activity with Cr load but this is not the case in the co-precipitated series. The most selective catalyst was the Cr1.0i.

Cr modifies the texture of the promoted VPO catalyst. The surface area increases and consequently the catalytic activity (Table 3), independent of the preparation method. This result is consistent with the data reported by Hutchings and Higgins [9] showing a significant increase in surface area with the addition of 1.0% of Cr. According to Hutchings, the increase in *n*-butane conversion upon Cr addition was directly connected to the higher surface area of their promoted catalyst. Note, however, that they only report data for one Cr load (Cr/V = 0.03). We would have reached the same conclusion if only one load of Cr had been used. But this claim

Table 2
Unit cell dimensions of the catalysts

Catalyst	Cell dimensions (Å)			Cell volume $(Å)^3$
	a	*b*	*c*	
VPO	7.703	9.552	16.522	1215.70
Cr0.5i	7.777	9.605	16.495	1232.21
Cr1.0i	7.721	9.612	16.619	1233.41
Cr1.5i	7.764	9.627	16.579	1239.18
Cr1.0c	7.632	9.563	16.577	1209.93
Cr1.5c	7.903	9.707	16.744	1284.57
Cr3.0c	7.584	9.717	16.553	1219.89

Table 3
Catalytic behavior and BET area[a]

Solids	BET Area ($m^2\ g^{-1}$)		*T* [80] (°C)[b]	*S* [80][c]
	Precursor	Catalyst		
VPO	11.0	28.21	445	50
Cr0.5i	11.0	44.62	440	50
Cr1.0i	13.0	46.20	427	70
Cr1.5i	12.0	44.32	405	43
Cr1.0c	11.0	45.33	430	23
Cr1.5c	12.0	48.13	435	53
Cr3.0c	11.0	35.00	440	25

[a] Activity and selectivity measured in a flow reactor at GHSV = 900 h^{-1}, feed stream 1.5% *n*-C_4H_{10} in air.
[b] Temperature at which the conversion reaches 80%.
[c] Selectivity measured at 80% conversion.

Table 1
Disorder and preferential exposure of the [2 0 0] plane

Solids[a]	Cr/V[b]	FWHM		Intensity ratios[c]	
		Precursor [0 0 1]	Catalyst [2 0 0]	Precursor I[0 0 1]/I[2 2 0]	Catalyst I[2 0 0]/I[0 4 2]
VPO	–	0.994	1.339	0.25	0.53
Cr0.5i	0.018	0.726	0.865	0.31	0.46
Cr1.0i	0.036	0.772	1.211	0.41	0.52
Cr1.5i	0.054	1.063	0.870	0.59	0.51
Cr1.0c	0.036	0.927	1.067	0.29	0.34
Cr1.5c	0.054	0.814	1.142	0.24	0.43
Cr3.0c[d]	0.108	0.225	0.245	0.67	–

[a] Promoter/percent weight/method of addition, i: impregnation, c: co-precipitation.
[b] Cr/V atomic ratio.
[c] Intensity ratio between planes [0 0 1] and [2 2 0] in the precursor and between [2 0 0] and [0 4 2] in the catalyst.
[d] This catalyst was the only one in which $(VO)_2P_2O_7$ was not the main phase.

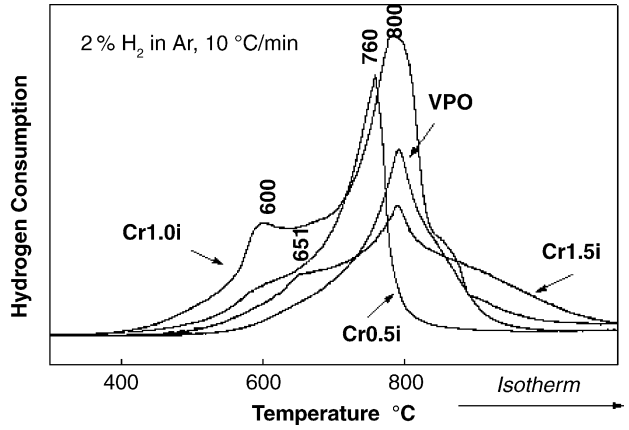

Fig. 1. Reduction profile of the Cr-impregnated catalysts.

cannot be sustained with our series because there is no correlation between Cr load, surface area and catalytic activity. So, other factors are playing a role in defining the catalytic activity (and selectivity) of the Cr promoted VPO catalysts. At this point, it should be recalled again that Cr-containing formulations catalyze the oxydehydrogenation of short chain paraffins. Both for this process and the oxidation of *n*-butane, the rate-determining step is the breaking of the C–H bond in the methylenic group (C_2–C_3) of the paraffin [14]. So, it seems reasonable to claim that the increased activity of the Cr-containing catalysts is due to the ability of this metal to increase the rate of C–H breaking. The most active catalysts were those obtained by impregnation and this may be due to better surface accessibility of the Cr added.

3.2. Reducibility of the used catalysts

In order to investigate whether or not Cr addition modifies the reducibility of the catalysts, TPR experiments were performed with all of them. Figs. 1 and 2 show the profiles obtained and Table 4 collects the H_2 consumed in each experiment. Note that in all cases, the main reduction peak appears around 800 °C (Figs. 1 and 2). Concerning $(VO)_2P_2O_7$ it has

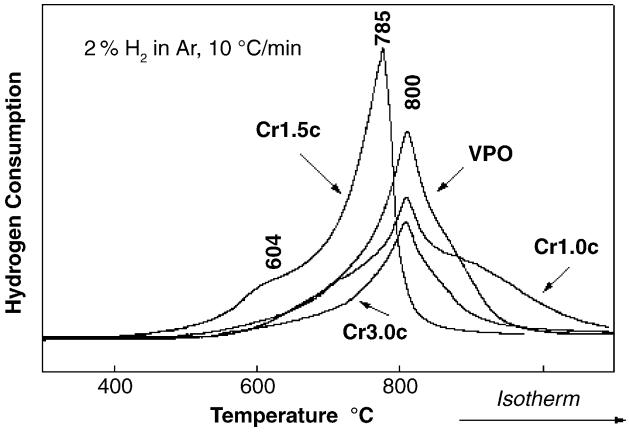

Fig. 2. Reduction profile of the Cr-co-precipitated catalysts.

Table 4
Hydrogen consumption for the different catalysts[a]

Catalyst	μmols of H_2	Ratio H_2/V[b]
VPO	252.34	0.364
Cr0.5i	264.82	0.382
Cr1.0i	550.33	0.795
Cr1.5i	317.97	0.459
Cr1.0c	250.22	0.361
Cr1.5c	245.88	0.355
Cr3.0c	147.78	0.213

[a] Catalyst mass: 100 mg; reductant mixture: 2% H_2 in Ar; rate of heating: 10 °C min^{-1}, from 40 to 800 °C.
[b] $H_2/V = 0.5$ means one electron reduction, V^{4+} to V^{3+}.

been reported by Tudo and Cartón [15] that it reduces to VPO_4 at temperatures between 600 and 800 °C. They used a mixture of 5% H_2 in N_2 and a heating rate of 2 °C min^{-1}. Note, that they started with an stoichiometric pyrophosphate while in our case we used an excess of 30% phosphorus (P/V = 1.3) This might explain why our unpromoted catalyst (VPO) was only partially reduced to an average oxidation state of 4.27 (Table 4).

In all the impregnated and Cr1.5c catalysts, a shoulder appears at temperatures between 600 and 650 °C. All the impregnated catalysts are easier to reduce than VPO but this effect does not occur with the co-precipitated ones. This is consistent with a higher surface exposure of Cr in the impregnated solids that could catalyze the reduction of vanadium. However, an unusual increase in H_2 consumption and a more prominent shoulder at 600 °C is observed in the case of Cr1.0i. The origin of this shoulder may be found in the presence of V^{5+} phases and/or dispersed V^{5+} being reduced to V^{4+}. Consequently, the higher H_2 consumption could be due to the additional reduction of V^{5+} to V^{3+}. Note, however, that the Cr3.0c which contains V^{5+} phases has a low H_2 consumption (Table 4).

An alternative explanation of the ca. 650 °C shoulder is the reduction of chromium species present in the catalysts, non-detectable by XRD. To check this option, the TPR profiles of Cr^{3+} and Cr^{6+} compounds were obtained (Fig. 3). Cr^{3+} was reduced to Cr^0 at 335 °C (Fig. 3A) and Cr^{6+} was reduced in two steps at much higher temperatures, 628 °C (Cr^{6+} to Cr^{3+}) and 713 °C (Cr^{3+} to Cr^0) (Fig. 3B). Thus, the results obtained do not seem to support the existence of highly dispersed Cr_2O_3 for no low temperature peaks are visible in Figs. 1 and 2. According to what is seen in Fig. 3B, if Cr^{6+} existed in the catalysts its peak would be buried under the vanadium reduction peaks. However, this would mean that during reaction Cr^{3+} has been oxidized to Cr^{6+}. Although this possible oxidation of Cr is hard to explain, our present data do not yield information enough to either prove or disprove this hypothesis.

Going back to the possible existence of a V^{5+} phase, the TPR profile of $VOPO_4{\cdot}2H_2O$ was obtained (Fig. 4). In view of the data obtained, we cannot exclude the possibility that the shoulder appearing at 600–650 °C in the promoted catalysts (Figs. 1 and 2) may be due to the presence of small amounts

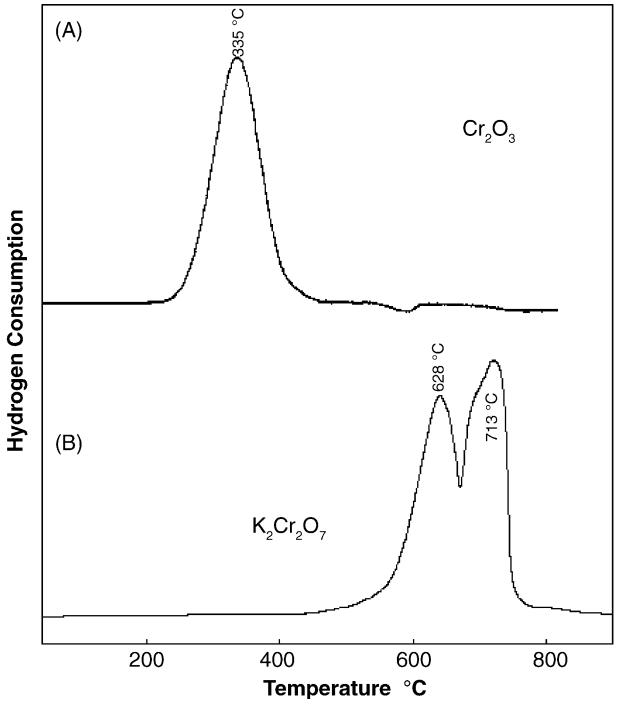

Fig. 3. Reduction profiles of Cr^{3+} oxide (A) and Cr^{6+} potassium di-chromate (B).

of V^{5+} phases. Again, note that this shoulder at lower temperatures and the H_2 consumption are particularly high for the Cr1.0i catalyst which contains γ-$VOPO_4$ (XRD patterns) and in turn is the second most active and the most selective formulation of all those studied here.

3.3. LRS data

This spectroscopic tool is especially suited to investigate the presence of different phases containing V, Cr and P oxides. Besides, it helps to detect small amounts of V^{5+}-containing phases buried in the predominant $(VO)_2P_2O_7$ crystalline phase. The spectra of the used catalysts show the characteristic fingerprints of $(VO)_2P_2O_7$ at 923, 1134 and 1178 cm^{-1}. These band assignments are taken from two independent

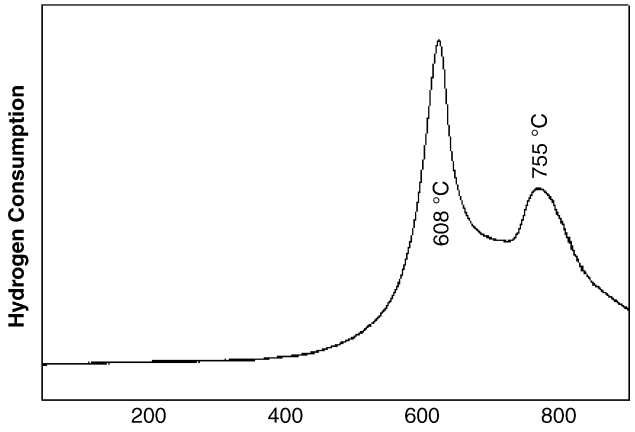

Fig. 4. TPR of hydrated vanadyl orthophosphate, $VOPO_4{\cdot}2H_2O$.

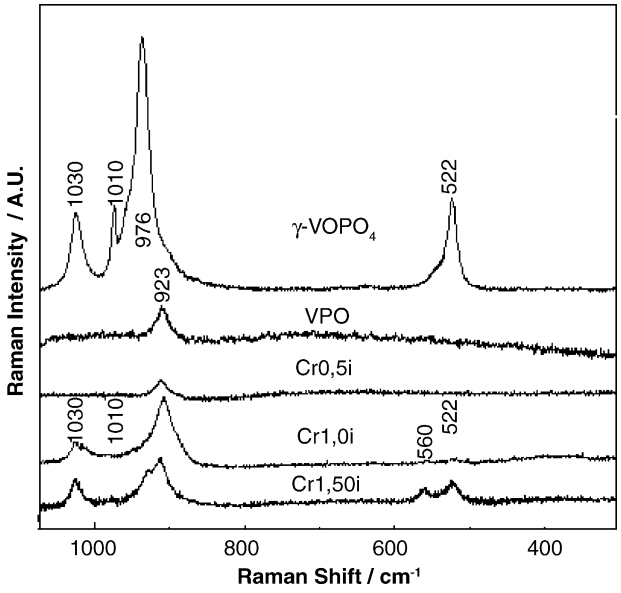

Fig. 5. Raman spectra of impregnated catalysts.

studies [16,17]. The spectra of the impregnated catalysts, the VPO base and the γ-$VOPO_4$ reference are shown in Fig. 5, while those of the coprecipitated catalysts are presented in Fig. 6.

The spectra of the catalysts Cr1.0i and Cr1.5i show one additional band at 1030 cm^{-1}. Besides, in the latter case, a shoulder appears at 976 cm^{-1} and two bands at 560 and 522 cm^{-1} (Fig. 5). The signals at 1030, 976 and 522 cm^{-1} could belong to γ-$VOPO_4$. In order to investigate the origin of the doublet at 560/522 cm^{-1}, the spectrum of Cr_2O_3 was recorded (Fig. 7). If the two bands are considered to come from the presence of both Cr_2O_3 and γ-$VOPO_4$, the I_{522}/I_{560} should be much higher than the ratio seen in the spectrum of Cr1.5i. So, no definite answer can be given to the presence of Cr_2O_3 in this solid.

The XRD data show the presence of γ-$VOPO_4$ in Cr1.0i but only the $(VO)_2P_2O_7$ reflections are seen in Cr1.5i. So, it is concluded that both chromium containing catalysts are made up of vanadyl pyrophosphate plus γ-$VOPO_4$. Besides, it is not possible to disregard the presence of very small crystals

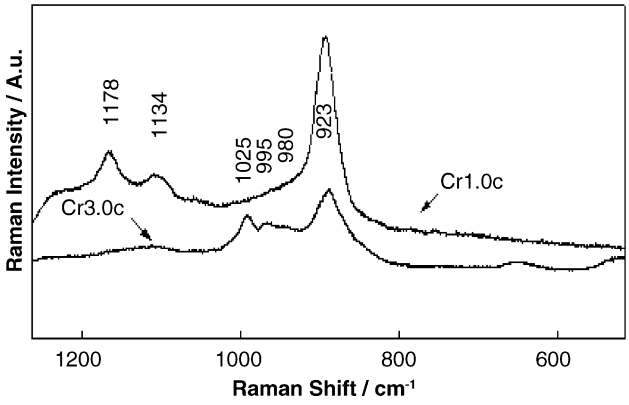

Fig. 6. Raman spectra of co-precipitated catalysts.

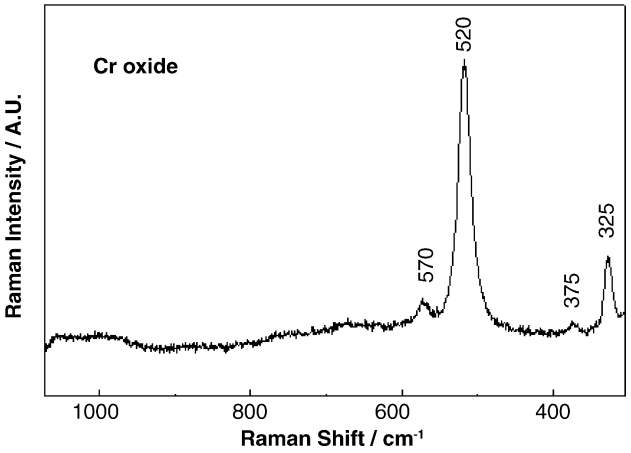

Fig. 7. Raman spectra of Cr_2O_3.

of Cr_2O_3 in the Cr1.5i catalyst, and less so at the surface level.

The Cr1.0c spectrum only shows the presence of vanadyl pyrophosphate (Fig. 6). An identical spectrum is obtained with Cr1.5c (not shown). On the other hand, the poorly crystallized Cr3.0c shows the presence of γ-$VOPO_4$ and a signal at 995 cm^{-1} which could belong to other V^{5+} phases (e.g. β-$VOPO_4$). The XRD data also show that a mixture of phases makes up this solid.

3.3.1. Broadening of the 923 cm^{-1} band

As seen in Figs. 5 and 6 this very strong signal significantly broadens upon addition of Cr. The width at half maximum of this signal has been collected in Table 5. For the base precursor without Cr added, the FWHM is 21 cm^{-1}, a value very close to the value we measured using highly crystalline $(VO)_2P_2O_7$ (20–22 cm^{-1}). When the V^{5+} phases are unmistakably identified, the peak width is about twice as big. However, when V^{5+} phases cannot be detected, one still sees a wide signal (ca. 30 cm^{-1}). It has been known for a long time that the vanadyl pyrophosphate lattice can admit up to 20% V^{5+} [18], without a significant displacement of the X-ray reflections. The only detectable feature is a broadening of the signals. In the same vein, Volta and coworkers [19,20] detected and measured the amount of highly dispersed V^{5+} sites in the pyrophosphate matrix using NMR techniques. Furthermore, in a joint work with our group [21] they measured the concentration of V^{5+} in the Co-promoted VPO catalyst which had been on stream over 800 h and which showed only the characteristic fingerprints of the vanadyl pyrophosphate (XRD and Raman). In view of this background information, in this work the widening of the 923 cm^{-1} band is taken as evidence of the presence of highly dispersed V^{5+} in the catalyst matrix.

Table 5
The presence of disperse V^{5+} in the $(VO)_2P_2O_7$ crystallite

Catalyst[a]	Other phases DRX[b]	Other phases Raman	FWHM 923 cm^{-1}
VPO			21[c]
Cr0.5i			31
Cr1.0i	(DH, γ)	(DH, γ)	46
Cr1.5i		(γ)	28
Cr1.0c	(DH)		35
Cr1.5c			35
Cr3.0c[d]	Phase mixture (DH, β)	Phase mixture[d]	42

[a] In all cases but the Cr3.0c the main phase is $(VO)_2P_2O_7$.
[b] (β, γ) $VOPO_4$: orthophosphates and (DH): $VOPO_4{\cdot}2H_2O$.
[c] For crystalline $(VO)_2P_2O_7$ the FWHM = 18–20 cm^{-1}.
[d] Only case where $(VO)_2P_2O_7$ is not the main phase.

3.4. FT-IR data

Through this spectroscopic technique, two goals were achieved: (i) to obtain additional structural information and (ii) to characterize the Lewis acidity of the catalysts using a weak base (acetonitrile) as a probe molecule.

3.4.1. Structural information

In the impregnated catalysts, there appears a strong band at 970 cm^{-1} [ν V(4+)=O] in the Cr1.0i catalyst while the other two do not show differences with the unpromoted catalyst (VPO). In all cases but one the band at 947 cm^{-1} pertaining to V^{5+} species is not visible. Not even an asymmetric broadening at the 970 cm^{-1} signal towards a lower wavenumber was detected in these solids. The characteristic bands corresponding to vanadyl pyrophosphate phases are: 970 (stretching of V=O), 742 (symmetric stretching of P–O–P bond). The intensity ratio of these bands is shown in Table 6. Only the Cr3.0c sample made up of a mixture of phases (XRD data) does not show this band.

The intensity ratio in the co-precipitated catalysts is significantly higher than in the VPO and the impregnated solids (Table 6). This could be due to the intercalation of Cr in the lattice, a bulk feature that is more likely to develop with co-precipitation than with impregnation.

3.4.2. Lewis acidity using acetonitrile

When this weak base is adsorbed, on a very strong Lewis acid, as $AlCl_3$, the νCN stretching frequency shifts to 2325 cm^{-1} from the liquid phase (or physisorbed) value of

Table 6
Relative values of the IR bands intensity ratios

Catalyst + KBr	Intensity ratio I(742)/I(970)[a]
VPO	0.041
Cr0.5i	0.052
Cr1.0i	0.030
Cr1.5i	0.062
Cr1.0c	0.091
Cr1.5c	0.078
Cr3.0c	NM

[a] The band at 970 cm^{-1} corresponds to the stretching mode of the V═O vibration and at 742 cm^{-1} it corresponds to the symmetric stretching of the P─O─P vibration.

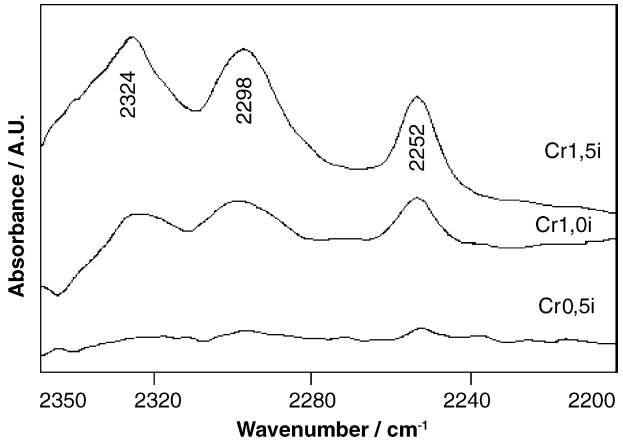

Fig. 8. FT-IR spectra of adsorbed acetonitrile over impregnated catalysts.

2252 cm^{-1}. When the adsorbent is a weaker acid such as ZnO and Fe_2O_3, the same signal moves to ca. 2280 cm^{-1} [21–23]. Fig. 8 shows the spectra obtained after acetonitrile adsorption on the impregnated catalysts. Three bands are clearly visible in the Cr1.0i and Cr1.5i at 2324 cm^{-1} (very strong Lewis acid sites), 2298 cm^{-1} (Fermi resonance band) and 2252 cm^{-1} physisorbed CH_3CN. The latter band rapidly disappears after evacuation at 30 °C. The co-precipitated and the VPO catalysts do not show the bands at 2324 cm^{-1}. Since these catalysts also produce maleic anhydride, this is probably due to the low concentration of very strong Lewis sites on those solids.

Table 7 shows the evolution of the peak area for the impregnated catalysts containing 1.0 and 1.5% of Cr. It is clear that these two catalysts contain very strong Lewis acid sites, the Cr1.5i being the most acidic one. Going back to Table 3, it is clearly seen that these two catalysts are the most active ones and particularly so the Cr1.5i. A significant difference in selectivity is seen in the same Table 3. The Cr1.0i is in fact the most selective of all the formulations assayed while the more acidic Cr1.5i is much less selective. This seems to indicate that there is an optimum acidity to maximize the maleic anhydride yield. The same conclusion was reached by Carrara et al. [2] when cobalt was the promoter.

Table 7
Intensity ratios of the characteristic bands of adsorbed ACN[a]

Step[b]	Area 2324	Area 2298	Area 2252	I(2324)/ I(2298)
Cr1.0i				
Adsorption 30 °C	0.572	0.547	0.576	1.045
Evacuation 30 °C	0.551	0.452	0	1.220
Evacuation 80 °C	0.207	0.308	0	0.672
Evacuation 150 °C	0	0.220	0	0
Cr1.5i				
Adsorption 30 °C	1.467	1.298	0.925	1.130
Evacuation 30 °C	0.509	0.459	0.0299	1.109
Evacuation 80 °C	0.441	0.421	0	1.045
Evacuation 150 °C	0.098	0.266	0	0.362

[a] 2324 cm^{-1}: very strong Lewis acids sites, 2298: Fermi resonance, 2252: CN stretching frequency of physisorbed base.
[b] In every case, the temperature at which the step was performed is indicated.

4. Conclusions

- Both the activity and selectivity of the catalysts are affected by the incorporation of Cr. Both effects are more pronounced in the impregnated catalysts (Table 3). There is an optimal concentration of Cr (1%), to obtain the best yield to maleic anhydride.
- The addition of Cr yields catalysts with ca. 50% higher surface area than the unpromoted VPO (Table 3). However, there is no correlation between surface area and Cr load. So the increase in activity obtained with Cr addition is not only attributable to this factor, as suggested by Hutchings and Higgins [9].
- The addition of Cr does not produce an increased preferential exposure of the [2 0 0] plane as reported for other promoters [24].
- $CrPO_4$ was not detected using bulk techniques so this does not discard the formation of this compound at the surface level.
- Cr favors the appearance of isolated V^{5+} species and in some cases V^{5+} containing phases. Particularly the formation of V^{5+}/V^{4+} couples could be a way to improve the catalyst selectivity.
- The catalysts obtained by impregnation are more acidic than those promoted by the co-precipitation method. The main effect of increasing the number of acid sites would be to increase the overall activity. Also the presence of small surface clusters of Cr_2O_3 may act in the same direction. But this could not be substantiated either by us or by other researchers. The best catalyst has an intermediate concentration of active sites (Cr1.0i). This may indicate that there is an optimum balance between acid site abundance and redox sites.

Acknowledgments

The authors wish to acknowledge the financial support received from UNL. They are also grateful to the Japan International Cooperation Agency (JICA) for the donation of the major instruments used in this study. Thanks are finally given to Prof. Elsa Grimaldi for the English language editing.

References

[1] V. Zazhigalov, J. Haber, J. Stoch, A. Pyatnizkaya, A. Komashko, V. Belousov, Appl. Catal. A 96 (1993) 153.
[2] C. Carrara, S. Irusta, E. Lombardo, L. Cornaglia, Appl. Catal. A 217 (2001) 275.
[3] G. Busca, G. Centi, F. Trifirò, Appl. Catal. 25 (1986) 265.
[4] G. Bergeret, M. David, J.P. Broyer, J.C. Volta, G. Hecquet, Catal. Today 1 (1987) 37.

[5] R. Mc Cormick, G. Alptekin, A. Herring, T. Ohno, S. Dec, J. Catal. 172 (1997) 160.
[6] B. Weckhuysen, R. Schoonheydt, Catal. Today 51 (1999) 223.
[7] N. Harrouch Batis, H. Batis, A. Ghobel, Appl. Catal. A: Gen. 147 (1996) 347.
[8] G. Hutchings, Appl. Catal. 72 (1991) 1.
[9] G. Hutchings, R. Higgins, J. Catal. 162 (1996) 153.
[10] E. Bordes, Catal. Today 1 (1987) 499.
[11] G. Centi, F. Trifirò, J. Ebner, V. Franchetti, Chem. Rev. 88 (1988) 55.
[12] E. Kesteman, M. Merzouki, B. Taouk, E. Bordes, R. Contractor, in: Poncelet, et al. (Eds.), Preparation of Catalysts VI, vol. 91, Stud. Surf. Sci. Catal. (1995) 707.
[13] N. Duvauchelle, E. Bordes, Catal. Lett. 57 (1999) 81.
[14] M. Pepera, J. Callahan, M. Desmond, E. Millberger, P. Blum, N. Bremer, J. Am. Chem. Soc. 107 (1985) 4883.
[15] J. Tudo, D. Cartón, C.R. Acad. Sci. Paris, Series C.V. 298 (1979) 219.
[16] F. Ben Abdelouhab, R. Olier, N. Guilhaume, F. Lefevre, J.C. Volta, J. Catal. 134 (1992) 151.
[17] V. Guliant, J. Benziger, S. Sunderesan, I. Wachs, J. Jehng, J. Roberts, Catal. Today 28 (1996) 275.
[18] G. Busca, F. Cavani, G. Centi, F. Trifiro, J. Catal. 99 (1986) 400.
[19] Y. Zhang-Lin, M. Forissier, R. Sneeden, J.C. Vedrine, J.C. Volta, J. Catal. 145 (1994) 267.
[20] M. Abon, J.M. Herrmann, J.C. Volta, Catal. Today 71 (2001) 121.
[21] L. Cornaglia, S. Irusta, E.A. Lombardo, M.C. Durupty, J.C. Volta, Catal. Today 78 (2003) 291.
[22] K. Purcell, R. Drago, J. Am. Chem Soc. 88 (1965) 919.
[23] G. Busca, G. Centi, F. Trifirò, J. Am. Chem. Soc. 107 (1985) 7758.
[24] D. Ye, A. Satsuma, A. Hattori, T. Hattori, Y. Murakami, Catal. Today 16 (1993) 113.